

## Calculating dilepton rates from Monte Carlo simulations of parton production

K. J. Eskola

*Nuclear Science Division, Mailstop 70A-3307, Lawrence Berkeley Laboratory,  
University of California, Berkeley, California 94720  
Laboratory of High Energy Physics, P.O. Box 9, SF-00014 University of Helsinki, Finland\**

Xin-Nian Wang

*Nuclear Science Division, Mailstop 70A-3307; Lawrence Berkeley Laboratory,  
University of California, Berkeley, California 94720*

(Received 18 October 1993)

To calculate dilepton rates in a Monte Carlo simulation of ultrarelativistic heavy ion collisions, one can scale the number of similar QCD processes by a ratio of the corresponding differential probabilities. We derive the formula for such a ratio especially for dilepton bremsstrahlung processes. We also discuss the non-triviality of including higher order corrections to the direct Drell-Yan process. The resultant mass spectra from our Monte Carlo simulation are consistent with the semianalytical calculation using dilepton fragmentation functions.

PACS number(s): 25.75.+r, 12.38.Bx, 13.87.Ce, 24.85.+p

### I. INTRODUCTION

In a previous paper [1], we investigated dilepton production associated with minijet final state radiation in heavy ion collisions at collider energies, using dilepton fragmentation functions which can be evaluated perturbatively. The dilepton pairs from the fragmentation of minijets are found to be comparable to the direct Drell-Yan (DY) processes for small invariant masses  $M \sim 1\text{--}2$  GeV/ $c^2$  at the highest energy of the Brookhaven Relativistic Heavy Ion Collider (RHIC). At the CERN Large Hadron Collider (LHC) energies, the associated dilepton production becomes dominant over a relative large range of the invariant mass.

Because of the relatively large invariant dilepton mass,  $M \gg \Lambda$ , the radiative corrections are calculable in perturbative QCD (PQCD) up to all orders in the leading logarithm approximation. The collinear approximation is also used in convoluting the obtained dilepton fragmentation functions with minijet cross sections to compute the radiative contributions to dilepton production. Since there exist Monte Carlo simulations of QCD cascading [2-4] which can take into account many other effects, such as the multiple ladder structure, it is important to check our semianalytical approach with realistic Monte Carlo simulations. In this way, we can address the validity of the approximations we made in the fragmentation function approach [1].

To directly simulate dilepton production in a Monte Carlo event generator is rather difficult due to the small QED coupling constant as compared to that of QCD. The simplest way to overcome this difficulty is to arti-

cially increase the QED coupling constant and normalize the result by a corresponding overall constant factor. However, one must make sure that the interactions are still overwhelmingly dominated by QCD processes with the increased QED coupling constant. Alternatively, one can also multiply the number of specific QCD processes, which resemble those of dilepton production, by an appropriate ratio of the corresponding differential probabilities. However, the problem is more complicated and was not discussed in Ref. [5]. For radiative dilepton production, one has to take into account the fact that the corresponding radiated quarks and gluons in QCD can have further bremsstrahlung which is different from the QED case. The additional bremsstrahlung gives rise to an extra Sudakov form factor and one must include it in the differential ratio to give the correct dilepton emission. We will derive a formula for the differential ratio and demonstrate that the resultant simulation is consistent with our previous semianalytical calculation in Ref. [1].

As is well known, coherence effects in QCD parton shower cause the angular ordering of the radiated partons [3], which will reduce the overall QCD emissions. Since QCD coherence is only relevant to radiation processes which have more than one QCD branching vertex, its influence on dilepton emission only comes through the second or higher order QCD corrections to the QED emission. As we have demonstrated in our previous paper [1], higher order QCD corrections to dilepton radiation are small. Therefore, we can neglect the influence of the coherence effects in QCD parton shower on dilepton emission rates.

The problem of simulating direct DY processes among QCD processes lies in how to take into account higher order  $O(\alpha^2\alpha_s)$  corrections. We will discuss when an overall  $K$  factor, as used in most Monte Carlo simulations of QCD hard processes in hadronic and nuclear collisions, is sufficient enough to simulate the QCD contributions.

\*Present address.

We also consider how possible double counting can be avoided.

The remainder of the paper is organized as follows. In the next section, we will discuss how to calculate the differential ratio to obtain dilepton emission from a Monte Carlo simulation of the corresponding PQCD processes. In Sec. III, we will discuss how to simulate direct DY processes, especially how to take into account higher order corrections. The results of our simulation will be compared to semianalytical calculations in Sec. IV, and finally, a summary with some discussions is given in Sec. V.

## II. SIMULATION OF DILEPTON BREMSSTRAHLUNG

If a Monte Carlo generator does not have the QED processes built in, one can calculate the absolute cross sections of the QED processes by scaling the differential cross sections of certain types of QCD processes. The scaling factor, however, depends on both the QED and QCD processes. For dilepton production through bremsstrahlung, one would naively think that a scaling factor between virtual photon and virtual gluon radiation processes from a quark line is enough. However, the probability to find a virtual gluon with fixed invariant mass depends on the probability that the gluon does not have any further radiations to degrade its virtuality. One therefore should use the scaling factor between process (a) and processes (b) and (c) in Fig. 1.

The Monte Carlo simulation of QCD cascading is carried out by giving for each vertex of the radiation tree, such as those in Fig. 1(b), a *normalized* probability distribution. Given the maximum virtuality  $Q_{\max}^2$  of a particular process, the normalized probability for the off-shell parton  $a$  with  $q^2 \leq Q_{\max}^2$  to branch into partons  $b$  and  $c$  of light-cone momentum fractions  $z$  and  $1-z$  is [2,3]

$$d\mathcal{P}_{a \rightarrow bc}(q^2, z) = \frac{dq^2}{q^2} dz P_{a \rightarrow bc}(z) \frac{\alpha_s [z(1-z)q^2]}{2\pi} \frac{\mathcal{S}_a(Q_{\max}^2)}{\mathcal{S}_a(q^2)}. \quad (1)$$

The relative transverse momentum between the radiated partons  $b$  and  $c$  is given by

$$q_T^2 = z(1-z) \left( q^2 - \frac{q_b^2}{z} - \frac{q_c^2}{1-z} \right). \quad (2)$$

$$\epsilon_{1,2}(q, M) = \frac{1}{2} \left[ 1 + \frac{M^2 - \mu_0^2}{q^2} \mp \sqrt{\left( 1 + \frac{M^2 - \mu_0^2}{q^2} \right)^2 - 4 \frac{M^2}{q^2}} \right]. \quad (5)$$

In Eq. (1), the Sudakov form factor  $\mathcal{S}_a(q^2)$  is defined as

$$\mathcal{S}_a(q^2) = \exp \left\{ - \int_{4\mu_0^2}^{q^2} \frac{dk^2}{k^2} \int_{\epsilon(k)}^{1-\epsilon(k)} dz \sum_{b,c} P_{a \rightarrow bc}(z) \frac{\alpha_s [z(1-z)k^2]}{2\pi} \right\}, \quad (6)$$

so that  $\mathcal{S}_a(Q_{\max}^2)/\mathcal{S}_a(q^2)$  is the probability for parton  $a$  not to have any branching between  $Q_{\max}^2$  and  $q^2$ . The contribution of QED processes to the Sudakov form factor is negligible.

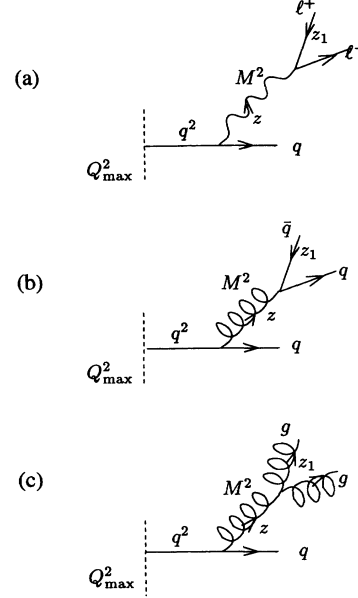


FIG. 1. Illustration of (a) dilepton, (b) quark-antiquark pair, and (c) two-gluon emission from a quark line. The dashed lines present the preceding radiation or scattering processes which kinematically determines the maximum value,  $Q_{\max}^2$ , of the quark virtuality  $q^2$ .

Note that the variable  $z(1-z)q^2$  in the strong coupling constant in Eq. (1) is approximately  $q_T^2$ . In a Monte Carlo simulation, the timelike branching is usually terminated at  $q^2 \leq \mu_0^2$ , where the physics of nonperturbative hadronization sets in. By requiring  $q_b^2, q_c^2 \geq \mu_0^2$  and the relative transverse momentum  $q_T$  to be real, one defines the kinematically allowed region of the phase space as

$$4\mu_0^2 < q^2 < Q_{\max}^2, \quad \epsilon(q) < z < 1 - \epsilon(q), \quad \epsilon(q) = \frac{1}{2} (1 - \sqrt{1 - 4\mu_0^2/q^2}). \quad (3)$$

If the virtuality of one of the radiated partons is fixed to  $q_b^2 = M^2$ , the above region of the phase space is modified to

$$(\mu_0 + M)^2 < q^2 < Q_{\max}^2, \quad \epsilon_1(q, M) < z < \epsilon_2(q, M), \quad (4)$$

where

Based on the above probability distributions, we can write down the differential probability for a quark to radiate either a  $q\bar{q}$  pair or two gluons via an intermediate virtual gluon with an invariant mass  $M$ , as shown in Figs. 1(b) and (c):

$$\begin{aligned} \frac{d\mathcal{P}_{q\rightarrow\text{all}}}{dM^2} &= \frac{1}{M^2} \int_{(M+\mu_0)^2}^{Q_{\text{max}}^2} \frac{dq^2}{q^2} \int_{\epsilon_1(q,M)}^{\epsilon_2(q,M)} dz P_{q\rightarrow gq}(z) \frac{\alpha_s[z(1-z)q^2]}{2\pi} \frac{\mathcal{S}_q(Q_{\text{max}}^2)}{\mathcal{S}_q(q^2)} \\ &\times \int_{\epsilon(M)}^{1-\epsilon(M)} dz_1 [n_f P_{g\rightarrow q\bar{q}}(z_1) + P_{g\rightarrow gg}(z_1)] \frac{\alpha_s[z_1(1-z_1)M^2]}{2\pi} \frac{\mathcal{S}_g((q-\mu_0)^2)}{\mathcal{S}_g(M^2)}. \end{aligned} \quad (7)$$

Notice the variables in the second set of Sudakov form factors. Since  $q^2$  is the actual virtuality of the quark line preceding the gluon radiation and the daughter quark line has at least virtuality of  $\mu_0^2$ , the maximum value of the gluon virtuality,  $M^2$ , is then  $(q-\mu_0)^2$ . Because of the same reason, the lower limit of the integration over  $q^2$  is  $(M+\mu_0)^2$ .

Similarly, the differential branching probability for the dilepton production via diagram (a) in Fig. 1 is

$$\frac{d\mathcal{P}_{q\rightarrow\text{dl}}}{dM^2} = \frac{e_q^2}{M^2} \int_{(M+\mu_0)^2}^{Q_{\text{max}}^2} \frac{dq^2}{q^2} \int_{\epsilon_1(q,M)}^{\epsilon_2(q,M)} dz P_{q\rightarrow\gamma q}(z) \frac{\alpha}{2\pi} \frac{\mathcal{S}_q(Q_{\text{max}}^2)}{\mathcal{S}_q(q^2)} \int_0^1 dz_1 P_{\gamma\rightarrow\ell^+\ell^-}(z_1) \frac{\alpha}{2\pi}, \quad (8)$$

where again we neglect the QED contribution to the Sudakov form factor, and the integration over  $z$  and  $z_1$  can be carried out analytically using Eq. (5). Notice that the differential probability for the dilepton bremsstrahlung has one Sudakov form factor less than the corresponding QCD processes. To obtain radiative dilepton production [Fig. 1(a)] by scaling the corresponding QCD processes [Figs. 1(b) and (c)], one simply multiplies the number of virtual gluons from a quark line by a ratio

$$\mathcal{R}(M^2, Q_{\text{max}}^2) \equiv \frac{d\mathcal{P}_{q\rightarrow\text{dl}}}{dM^2} \bigg/ \frac{d\mathcal{P}_{q\rightarrow\text{all}}}{dM^2}, \quad (9)$$

for given  $M^2$  and  $Q_{\text{max}}^2$ .

To demonstrate the effects of the Sudakov form factor on scaling QCD processes of the Monte Carlo simulations, we plot in Fig. 2 the ratio  $\mathcal{R}(M^2, Q_{\text{max}}^2)$  (solid line) as a function of  $Q_{\text{max}}$  at fixed  $M = 2 \text{ GeV}/c^2$  to-

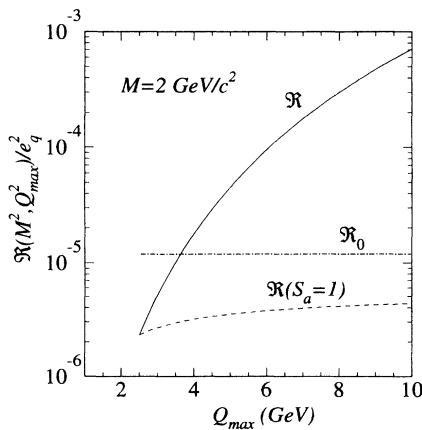


FIG. 2. The ratio  $\mathcal{R}(M^2, Q_{\text{max}}^2)$  between the probability of  $q \rightarrow \ell^+\ell^- + q$  and  $q \rightarrow q_i\bar{q}_i + q$ ,  $gg + q$  processes as functions of  $Q_{\text{max}}$  at fixed  $M = 2 \text{ GeV}/c^2$ , with (solid line) and without (dashed line) the Sudakov form factors.  $\mathcal{R}_0$  (dot-dashed line) is obtained with both Sudakov form factors and the  $z(1-z)q^2$  dependence of  $\alpha_s$  neglected. A factor  $e_q^2$  is divided out.

gether with the result (dashed line) obtained when Sudakov form factors are set to unity. We also show the value of  $\mathcal{R}_0(M^2, Q_{\text{max}}^2)$  (dot-dashed line) in which both the Sudakov form factors and  $z(1-z)q^2$  dependence of the coupling constant are neglected. In this case the ratio is reduced to

$$\mathcal{R}_0(M^2, Q_{\text{max}}^2) = \frac{e_q^2}{2\gamma_g(M)} \frac{\alpha^2}{\alpha_s(M)^2}, \quad (10)$$

which is independent of  $Q_{\text{max}}$ , and where

$$\begin{aligned} \gamma_g(M) &\equiv \int_{\epsilon(M)}^{1-\epsilon(M)} dz [n_f P_{g\rightarrow q\bar{q}}(z) + P_{g\rightarrow gg}(z)] \\ &= 6 \ln[1/\epsilon(M) - 1] + 9[\epsilon(M) - \frac{1}{2}]. \end{aligned} \quad (11)$$

Since a Sudakov form factor takes into account additional branchings preceding the chosen vertex, it should suppress the probability distribution of the splitting  $g \rightarrow q\bar{q}, gg$  at the given  $M$ . As we see in Fig. 2, the ratio  $\mathcal{R}(M^2, Q_{\text{max}}^2)$  is therefore enhanced relative to both the case when  $\mathcal{S}_a = 1$  and to  $\mathcal{R}_0(M^2, Q_{\text{max}}^2)$  by the inclusion of Sudakov form factors. The enhancement increases with  $Q_{\text{max}}$  as expected due to the increasing branching probability. Similar to the dilepton fragmentation functions, the ratio is very sensitive to the scale  $Q_{\text{max}}$ . We will discuss in Sec. IV how we choose  $Q_{\text{max}}$  which is consistent with the Monte Carlo simulation of QCD cascading. When Sudakov form factors are set to unity, the dependence of the ratio on  $Q_{\text{max}}$  only comes from the  $z$  and  $q^2$  dependence of the running strong coupling constant. If both  $z(1-z)q^2$  and  $z_1(1-z_1)M^2$  in Eq. (7) are replaced by  $M^2$ , the ratio  $\mathcal{R}_0$  becomes larger and is independent of  $Q_{\text{max}}$  as shown in Fig. 2.

The purpose of the ratio in Eq. (9) is to cancel whatever the probability for a virtual gluon emission used in the parton shower simulation and replace it by that for a virtual photon radiation. Since Sudakov form factors are used in our parton shower simulation, we find it essential to include the Sudakov form factors in the calculation of

the ratio in order to obtain the dilepton rates consistent with our semianalytical results [1].

### III. SIMULATION OF DIRECT DY PROCESSES

It is relatively easier to simulate the lowest order process of direct Drell-Yan processes by multiplying the differential cross section of  $q\bar{q} \rightarrow q_i\bar{q}_i, gg$  by the ratio

$$\mathcal{R}_{\text{DY}} = \frac{d\sigma_{q\bar{q} \rightarrow \text{DY}}}{\sum_{i=1}^{n_f} d\sigma_{q\bar{q} \rightarrow q_i\bar{q}_i} + d\sigma_{q\bar{q} \rightarrow gg}}. \quad (12)$$

It is more subtle, however, to include QCD corrections. These higher order corrections which give rise to a so-called  $K$  factor have been studied extensively [6]. The problem here is how to include this  $K$  factor in scaling QCD processes to obtain the DY cross sections.

The first order correction to DY process in QCD comes from the ‘‘annihilation’’  $q\bar{q} \rightarrow g + \text{DY}$ , the ‘‘Compton’’  $q + g \rightarrow q + \text{DY}$  process, and the virtual corrections [6]. Like in deeply inelastic lepton nucleon scattering (DIS), there are infrared singular and finite contributions from these corrections. The infrared singular and part of the finite terms can be absorbed into the quark and anti-quark distribution functions which are defined in DIS processes and should be evaluated at the scale of  $M^2$  according to Altarelli-Parisi evolution equations [7]. What are left over are finite and scheme-independent contributions from the higher order corrections. One can find detailed discussions in, e.g., Ref. [8]. What we want to point out here is that the dominant contribution to the  $K$  factor of about 2 in the ( $p_T$ -integrated) mass spectrum of the direct DY process is from the virtual corrections. The contributions from real corrections which depend on both the quark and gluon distribution functions are relatively very small. Therefore, as a first approximation, we can include higher order corrections to direct DY process in our simulation by multiplying the QCD cross sections of  $q\bar{q} \rightarrow q_i\bar{q}_i, gg$  by an effective  $K = 2$  factor. This  $K$  factor in principle now includes both real and virtual corrections. The quark distribution functions in the cross section should be evolved and evaluated at scale  $M^2$ .

In the Monte Carlo simulations, one could also include the real QCD corrections explicitly to DY processes by counting the number of similar QCD processes,  $q\bar{q} \rightarrow gg, q + g \rightarrow q + g$  and scaling them by some calculable ratio as has been done in Ref. [5]. However, one still has to include the virtual corrections which can be characterized as an effective multiplicative factor, but which now differs from the normal overall DY  $K$  factor. This is exactly the problem one has to face if one wants to simulate the  $p_T$  distribution of DY dilepton pairs, whose large  $p_T$  tail mainly comes from real QCD corrections. The lowest order DY process only contributes to the small  $p_T$  part of the spectrum by including the intrinsic  $p_T$  of quarks and antiquarks. The virtual corrections to the lowest order DY can be taken into account by using an effective  $K$  factor. However, one must be very careful not to include the real corrections in this effective  $K$  factor.

In the Monte Carlo simulations of QCD processes in

hadronic collisions, one usually also uses an effective  $K$  factor to take into account higher order corrections [4]. However, this  $K$  factor should not be included when one scales the number of  $q\bar{q} \rightarrow gg$  and  $q + g \rightarrow q + g$  processes by some ratio to calculate the real QCD corrections to the DY process. Otherwise, double counting may occur.

### IV. NUMERICAL RESULTS

To perform the Monte Carlo simulations, we use PYTHIA [4] subroutines for QCD hard scatterings and the associated bremsstrahlungs as adapted in HIJING model [9]. HIJING is a Monte Carlo model developed for parton and particle production in high energy  $pp, pA$ , and  $AA$  collisions. In this model, multiple minijet production at  $NN$  level is calculated in the eikonal formalism [10]. As in many other models which attempt to merge low and high  $p_T$  dynamics, a  $p_T$  cutoff scale  $p_0$  has to be introduced, which will limit the invariant masses of produced dileptons in our simulation. For nuclear interactions, binary approximation is assumed for independent hard scatterings. Jet quenching due to final state interaction of produced partons with a stringlike soft mean field was also included in the original HIJING model [11]. We switch off these final state interactions to simplify our study here so that we can compare the numerical results with semianalytical calculations. The initial parton distribution functions of a nucleon are taken to be Duke-Owens parametrization [12] set 1. Nuclear shadowing and its scale dependence are also taken into account as in Ref. [13]. The impact parameter dependence of the nuclear parton distributions is modeled in according to Refs. [9,14]. However, at  $\sqrt{s} = 200A$  GeV, the shadowing effects on the associated dilepton production are small as seen in Ref. [1].

During the final state radiation, we count the number of virtual gluons with given invariant mass  $M$  which are radiated from quark lines. The maximum virtuality  $Q_{\text{max}}$  of the quark should be the invariant mass of its parent parton minus the minimum virtuality  $\mu_0$  of its sister parton. If there is no bremsstrahlung prior to this branching vertex,  $Q_{\text{max}}^2$  should be related to the transverse momentum transfer  $p_T$  of the corresponding hard scattering. In order to conserve both energy and momentum, the two produced partons from a hard scattering are combined together in PYTHIA [15] to initiate final state radiation. The total virtuality of the two-parton system is chosen to be  $2p_T$ . Since both of the partons must have at least a virtuality of  $\mu_0$ , the maximum virtuality of the selected quark immediately after the hard scattering should be  $Q_{\text{max}} = 2p_T - \mu_0$ . With given  $M^2$  and  $Q_{\text{max}}^2$ , we then can calculate the number of dileptons produced from the final state radiation by multiplying the number of these radiated virtual gluons with the ratio  $\mathcal{R}(M^2, Q_{\text{max}}^2)$ . Shown by the solid histogram in Fig. 3 is the invariant mass distribution of the radiated dileptons thus obtained for central Au+Au collisions at RHIC energy. In the simulations, the parton shower is terminated whenever a minimum virtuality  $\mu_0 = 0.5$  GeV is reached. Then the parton is put on shell and considered real. So

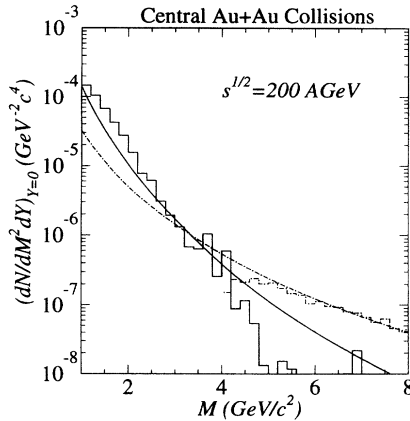


FIG. 3. Mass spectrum of the minijet-associated (solid histogram) and direct DY (dashed histogram) dileptons from the Monte Carlo simulation and our direct calculation (solid and dashed curves, respectively) (with  $Q_{\max} = 2p_T$ ,  $\Lambda = 0.4$  GeV, and  $\mu_0 = 0.5$  GeV) in central Au+Au collisions at  $\sqrt{s} = 200A$  GeV.

the minimum invariant mass of our selected virtual gluons, thus also of the dileptons, is  $2\mu_0 = 1$  GeV, according to Eq. (3).

We also plot in Fig. 3 our semianalytical calculation of the radiative dilepton production (solid curve) which agrees quite well with the simulated result. The small differences both in the total number and the slope of the distribution could come from several simplifications we made in our semianalytical approach. As stated in Ref. [1], we did not fully take into account the kinematic restrictions [Eqs. (3,5)] at every stage of the radiation tree in the calculation of the dilepton fragmentation functions. The variable in the strong coupling constant is taken to be  $q^2$  instead of the relative transverse momentum  $q_T^2 \approx z(1-z)q^2$ . The fragmentation function approach has only one branching tree corresponding to a simple ladder structure, whereas the Monte Carlo simulation takes into account all possible branching trees, thereby enhancing the small  $M$  dilepton production. In order to be as consistent as possible in both calculations in Fig. 3, we have chosen the same scales  $Q_{\max} = 2p_T$  and  $\Lambda = 0.4$  GeV in the dilepton fragmentation functions as have been used in the Monte Carlo simulations [4].

To simulate the lowest order direct DY processes, we simply count the number of similar QCD subprocesses,  $q\bar{q} \rightarrow q\bar{q}$ ,  $gg \rightarrow q\bar{q}$  at fixed  $\hat{s} = M^2$ . We then multiply the number by the ratio  $\mathcal{R}_{\text{DY}}$  to obtain the number of direct DY dileptons, which is shown as the dashed histogram in Fig. 3. We also compare the result to the parton model calculation (dashed curve) with the same set of parton distribution functions as used in the simulation. Higher order corrections are included by multiplying a  $K = 2$  factor in both the simulation and analytical calculation. In terms of  $p_T$  and rapidities  $y_{1,2}$  of minijets, the invariant mass of the dilepton is

$$M^2 = 2p_T^2[1 + \cosh(y_1 - y_2)]. \quad (13)$$

Since we have a cutoff  $p_0 = 2$  GeV/c for  $p_T$ , the lower

limit of the dilepton mass from the Monte Carlo simulation is then  $M \leq 4$  GeV/c<sup>2</sup>. The analytical calculation can go as low as the initial scale of the structure functions,  $Q_0 = 2$  GeV.

## V. CONCLUSIONS

In this paper, we have studied minijet-associated dilepton production in ultrarelativistic nuclear collisions through Monte Carlo simulations to check our previous semianalytical calculation [1] through the fragmentation function approach. We derived a formula for the differential ratio by which we multiply the number of similar QCD processes to obtain dilepton production from the Monte Carlo simulations of QCD cascading. Using this ratio, we found that our semianalytical calculation is consistent with Monte Carlo simulations. The difference between the two due to some simplifications we made in the fragmentation function approach is small.

Most importantly, we found that Sudakov form factors are essential for us to give the right results. If neglected, the resultant dilepton rate from final state radiation would differ from our early semianalytical calculation by orders of magnitude. For the same reason, the differential ratio is quite sensitive to the maximum virtuality  $Q_{\max}$  of the branching processes, similar to the fragmentation function approach. One therefore has to choose its value to be consistent with what is used in the Monte Carlo simulation of QCD cascading.

We also simulated the direct Drell-Yan processes of dilepton production and compared it to semianalytical calculation in the parton model. We pointed out the complication in including higher order corrections in the Monte Carlo simulations and the possibility of double counting. We believe this is especially important when one wants to simulate dilepton production through the final state parton rescatterings [5,16] in a dense partonic system such as quark-gluon plasma. Unlike in hadronic scatterings where infrared singularities due to real and virtual corrections can be absorbed into the definition of QCD evolved parton distribution functions, the screening mass due to resummation of hot thermal loops [17] naturally regulates the infrared divergences. However, one still has important contributions from both real and virtual corrections [18]. In order to take into account these corrections in a Monte Carlo simulation, one needs to analyze the higher order calculation in finite temperature QCD in detail.

## ACKNOWLEDGMENTS

This work was supported by the Director, Office of Energy Research, Division of Nuclear Physics of the Office of High Energy and Nuclear Physics of the U.S. Department of Energy under Contract No. DE-AC03-76SF00098. K.J.E. thanks Magnus Ehrnrooth foundation, Oskar Öflund foundation, and Suomen Kulttuurirahasto for partial financial support.

- [1] K. J. Eskola and X.-N. Wang, preceding paper, Phys. Rev. D **49**, 4532 (1994).
- [2] R. Odorico, Nucl. Phys. **B172**, 157 (1980).
- [3] G. Marchesini and B. R. Webber, Nucl. Phys. **B238**, 1 (1984).
- [4] T. Sjöstrand, Comput. Phys. Commun. **39**, 347 (1986); T. Sjöstrand and M. Bengtsson, *ibid.* **43**, 367 (1987).
- [5] K. Geiger and J. I. Kapusta, Phys. Rev. Lett. **70**, 1920 (1993).
- [6] G. Altarelli, R. K. Ellis, and G. Martinelli, Nucl. Phys. **B157**, 461 (1979); J. Kubar, M. Le Bellac, J. L. Meunier, and G. Plaut, *ibid.* **B175**, 251 (1980); F. Khalafi and W. J. Stirling, Z. Phys. C **18**, 315 (1983).
- [7] G. Altarelli and G. Parisi, Nucl. Phys. **B126**, 298 (1977).
- [8] See, e.g., R. D. Field, *Applications of Perturbative QCD*, Frontiers in Physics, Vol. 77 (Addison-Wesley, Reading, MA, 1989).
- [9] X.-N. Wang and M. Gyulassy, Phys. Rev. D **44**, 3501 (1991); **45**, 844 (1992).
- [10] X.-N. Wang, Phys. Rev. D **43**, 104 (1991).
- [11] X.-N. Wang and M. Gyulassy, Phys. Rev. Lett. **68**, 1480 (1992).
- [12] D. W. Duke and J. F. Owens, Phys. Rev. D **30**, 50 (1984).
- [13] K. J. Eskola, Nucl. Phys. **B400**, 240 (1993).
- [14] K. J. Eskola, Z. Phys. C **51**, 633 (1991).
- [15] T. Sjöstrand, Report No. CERN-TH.6488/92 (unpublished).
- [16] I. Kawrakow, H.-J. Möhring, and J. Ranft, in *Quark Matter '91*, Proceedings of the Ninth International Conference on Ultrarelativistic Nucleus-Nucleus Collisions, Gatlinburg, Tennessee, edited by T. A. Awes *et al.* [Nucl. Phys. **A544**, 471c (1992)].
- [17] E. Braaten and R. D. Pisarski, Nucl. Phys. **B337**, 569 (1990).
- [18] T. Altherr and P. V. Ruuskanen, Nucl. Phys. **B380**, 377 (1992).